Anomalous structural feature of $LiNbO_3$ observed using neutron diffraction

R. Fernández-Ruiz,[1] D. Martín y Marero,[2] and V. Bermúdez[1,*]
[1]*Departamento Física de Materiales, Universidad Autónoma de Madrid 28049, Spain*
[2]*Centro de Microanálisis de Materiales (Laboratorio del Acelerador), Universidad Autónoma de Madrid, 28049 Madrid, Spain and Institut Laue-Langevin, 6 rue Jules Horowitz, 38042 Grenoble, Rhone-Alpes, France*
(Received 18 January 2005; revised manuscript received 25 July 2005; published 30 November 2005)

An anomalous structural effect has been observed and analyzed on $LiNbO_3$ at low temperature by neutron-diffraction experiments. Two minima in the unit-cell volume at 55 and 100 K related with maxima and minima in the volume vibrational isotropic factors of Li and Nb atoms, respectively, and a change in the curve slope of the spontaneous stress at 55 K have been identified. This fact, together with the shortening in distance of the Li and O layers at 55 K, has been related with variations in the Ps factor through the secondary pyroelectric effect.

DOI: 10.1103/PhysRevB.72.184108 PACS number(s): 77.84.Dy, 61.12.−q, 77.80.Bh

Optoelectronics, acoustoelectronics, and photonics are continuously demanding new materials due to their fast development. In most of the cases, better than developing a new material, it is required to successfully modify those parameters of well-known materials. However, the lack of knowledge on the complicated relationship between lattice site location and physical properties of the material obviously limits our abilities to overcome drawback materials characteristics for entirely fitting the specified industrial requirements.

Lithium niobate has been described as a decathlon winner in photonics,[1] not the best for each application but the most complete to be used for industrial purposes. Lithium niobate (LN) has been extensively studied at high temperatures (from room to melting temperature) and although several efforts have been made to understand its intrinsic lattice characteristics,[2–6] some phenomena are still not comprehended. In fact, there is a lack of knowledge in material properties at low temperature. In particular, LN has been extensively studied in the range of very low temperature.[7–10] However, to our knowledge, few detailed structural studies are available below 77 K.

In the ferroelectric phase, at room temperature, LN exhibits threefold rotation symmetry about the *c* axis within a trigonal crystal system. In addition, it exhibits mirror symmetry about three planes that are 60° apart and intersect forming a threefold rotation axis.[11] These two symmetry operations classify LN as a member of the 3*m* point group. This structure is the only one present until the ferroelectric phase transition takes place at 1210 °C, only 50 °C below melting temperature. No more phase transitions have been identified in LN.

LN structure has been described as a very distorted perovskite with a tilt rotation of the oxygen triangles around the *c* axis. In the ferroelectric phase it exhibits both cation (Li and Nb) shift along [001] and octahedral tilt about [001]. As temperature approaches the transition temperature, octahedral cations diminish their shift, octahedral tilts disappear, and LN goes into the cubic perovskite. The ionic displacements of Li and Nb ions in the ferroelectric phase implies that to achieve the paraelectric phase it is necessary that Li and Nb ions experience a displacement from their equilibrium position in the ferroelectric phase. This sequence of loss of spontaneous polarization with increasing temperature gives LN its large pyroelectric coefficient dP/dt. It is important to remark on the high volume vibrational isotropic factor of Li ions. This fact indicates that the Li ion is allowed to vibrate in a high volume region of the oxygen octahedral. It is worthy to note that the origin of the tilt angle rotation of the oxygen triangles has not yet been identified.

LN is a congruently nonstoichiometric grown material, which means that congruent composition differs from the stoichiometric one. Nonstoichiometric composition implies the existence of structural vacancies in the LN lattice. To describe the LN structure by compensating charge, to guarantee charge neutrality, different defect models have been described, being the most simple lithium vacancy, niobium vacancy, and oxygen vacancies. These models have been fully described in Ref. 5. In the present work we will assume the Li vacancy model for calculations, where Li vacancies are compensated by Nb antisites. In this sense, we performed Rietveld refinements for different model vacancies and no difference in the overall behavior was observed. But a deep study of refining parameters with a defect model indicated that the model which minimizes Rietveld parameters was the Li vacancies one, as will be published elsewhere.

Noncongruent $LiNbO_3$ crystals have been grown in the Crystal Growth Laboratory in the Universidad Autónoma de Madrid, by the top seeded solution growth method.[12] Li composition was measured with inductively coupled plasma-mass spectrometry,[13] and indirect techniques as indicated in Ref. 12. In order to exactly determine the structural characteristics of noncongruent LN crystals and its behavior as a function of temperature, neutron diffraction at low-temperature experiments were carried out at ILL, Grenoble (France) using the D1B and D1A neutron diffractometers.[14] The low atomic number of Li and the vacancy model assumed in this work have determined the radiation used as a probe.

D1B is a medium flux and medium resolution diffractometer which allows rather fast data acquisition, ideal for parametric studies. It has a position sensitive detector (400 ^{3}He cells) with an angular coverage of 80 ° and 0.2 ° angular resolution, which can be moved to cover the $2° < 2\theta$

$<160°$ range. For this work, the wavelength of 2.52 Å reflected by the pyrolitic graphite (PG) monochromator was used and the "banana" was positioned to start at 35 °. D1A is a low flux and high-resolution diffractometer ideal for the determination of structural parameters. It has 25 ^{3}He detectors that can sweep to cover the $2°<2\theta<160°$ range in steps of 0.05 °. A wavelength of 1.904 A was chosen for this experiment. The almost perfect Gaussian peak shape of D1A is ideal for the Rietveld refinement method. For these measurements the grown $LiNbO_3$ crystals were reduced to powder and a 6-mm-diameter vanadium cell was used as container. The temperature ranges were obtained with a standard orange cryostat on D1B and the standard displex of D1A.

The data analysis of the above-mentioned diffraction patterns was performed following the Rietveld refinement[15] method with the FULLPROF suite of programs.[16] The basic lines followed in this process are adjusted to the proposals by McCusker *et al.* in the paper "Rietveld Refinements Guidelines".[17] During the analysis and to take into account the experimental conditions, the coefficients of the instrumental resolution function (IRF) in Cagliotti's equation[18] $\mathrm{FWHM}^2(\theta)=Utg^2\theta+Vtg\theta+W$, where FWHM is full width at half maximum, had to be modified from their theoretical values. The fitted final values were $U=0.0525$, $V=-0.1703$, $W=0.1463$ for the D1A-Ge (115) monochromator and $U=1.231\,12$, $V=-0.753\,56$, $W=0.091\,76$ for the D1B-PG (002) crystal. During these studies, we came out with the observation of an interesting physical effect at around 60 K for near congruent crystals with a 48.98%-mol Li composition, which means $x=0.0067$ for Eq. (1). Other compositions and a comparison with the one shown in this work are to be published elsewhere.

For the Rietveld refinement, 17 parameters were left free, 8 structural and 9 from diffraction peaks profile. To fit the peaks we used a pseudo-Voigt function $pV(x)$, defined as a Lorentzian $L(x)$ and a Gaussian $G(x)$ function of the mixing parameter η, as it is shown in $pV(x)=\eta L(x)+(1-\eta)G(x)$, where $\eta=\eta_0+X2\theta$; $0\leqslant\eta\leqslant1$, and X is a parameter to refine, $G(x)=a_G\exp(-b_Gx^2)$, $L(x)=a_L/(1+b_Lx^2)$, $a_G=(2/H)\sqrt{\ln 2/\pi}$, $b_G=4\ln 2/H^2$, $a_L=2/\pi H$, $b_L=4/H^2$, and H is the same FWHM for $G(x)$ and $L(x)$.

Using this procedure physical inconsistencies appeared, such as negative isotropic thermal parameters for Nb, Li, or O and negative FWHM in the diffraction lines. Therefore some parameters were fixed: the isotropic thermal factors $B_{\mathrm{Nb}}=0.43$, $B_{\mathrm{Li}}=0.5$, $B_{\mathrm{O}}=0.48$; the Cagliotti parameters $U=1.231\,12$, $V=-0.753\,56$, $W=0.091\,76$; and the Nb occupancy $O_{\mathrm{Nb}}=1.00$. Nb occupancy was also fixed due to the FULLPROF program requirements. The model defects of LN used for Rietveld refinement was −Li/Nb-Li with a chemical equation:

$$[\mathrm{Li}_{1-5x}\mathrm{Nb}_{x\ 1-4x}]_{Li}[\mathrm{Nb}]_{Nb}[\ ]_{\diamond}[\mathrm{O}_3]_O, \qquad (1)$$

where $[\ ]_{\diamond}$ is the sublattice of octahedral holes, □ are the Li vacancies, and Li vacancies compensated by Nb in Li positions are assumed. This has been done in this way due to the fact that a deep study of model defects considering Rietveld refining parameters indicated that Li vacancy model was adequate.

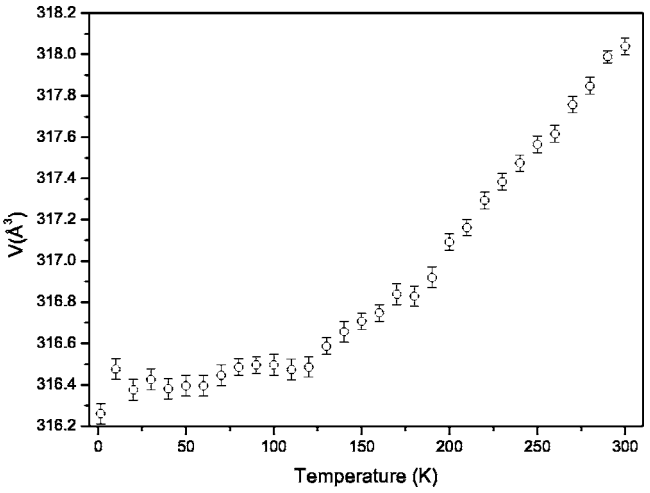

FIG. 1. Variation of the $LiNbO_3$ cell volume versus temperature on the D1B neutron beamline.

After refinements we obtained the lattice parameters and thus the volume of the unit cell as a function of the sample temperature. Figure 1 shows this behavior.

Here we can observe that an interesting phenomenon in LN is present. In this figure the volume of the unit cell is smoothly changing with temperature exhibiting at least two clearly identified local minima around 55 and 100 K. Two other dips can be observed around 20 and 200 K. To verify the above results, these measurements were repeated at a higher resolution on the D1A beamline using a totally different cryogenic and detection system.

After Rietveld refinement of the neutron-diffraction patterns obtained from neutron-diffraction patterns of the D1A beamline, the lattice parameters and the unit-cell volume were calculated. These results are displayed in Fig. 2, where the unit-cell volume versus temperature is shown.

The first thing we can observe in this figure is the fact that dips around 20 and 200 K have disappeared. This fact we assumed is due to the best instrumental resolution and thermal stability obtained in the measures with the D1A beamline. Looking closely at the low-temperature region in Fig. 2(a), 10–110 K, we observe that the two local minima around 55 and 100 K are better defined than in Fig. 1. Figure 2(b) shows the zoom of this low-temperature region where these two local minima at 55 and 100 K appear. The minimum around 100 K can be correlated with the change in the slope curve related with the typical change in the dilatation coefficient with increasing temperature, while the minimum at 55 K is a nonpreviously reported anomalous structural effect. However, no apparent change in the ferroelectric phase $LiNbO_3$ space group has been identified. Thus, we cannot attribute this effect at a second-order phase transition.

To eliminate possible random causes originating from this behavior as an artefact during the Rietveld refinement procedure, we performed several mathematical controls. We checked the effect of sample thermal stability, the effects of mathematical correlation in the multiple Rietveld refinements, we verified the appearance of this phenomenon in

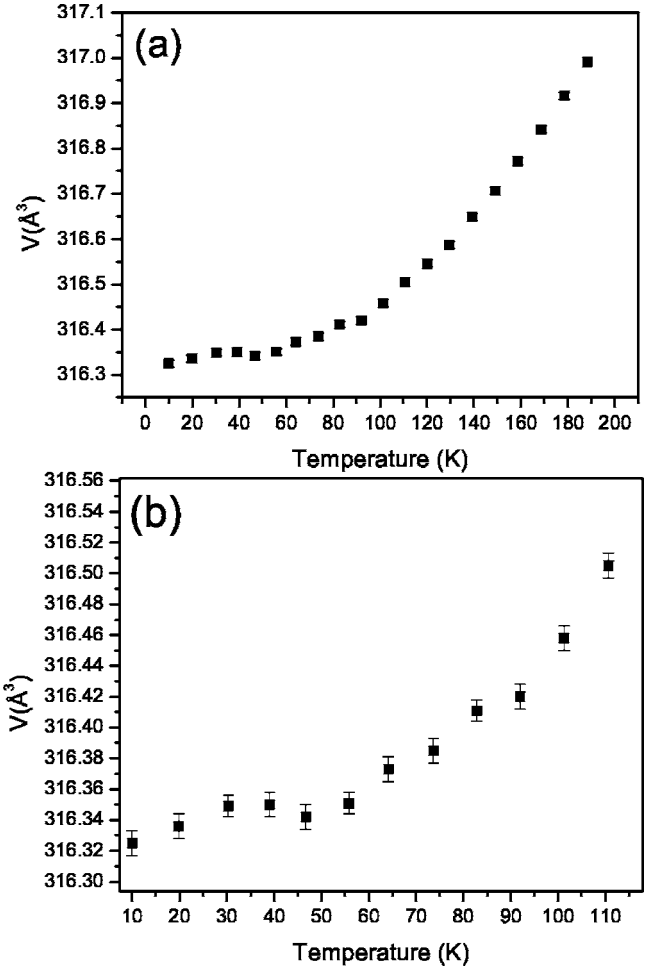

FIG. 2. Variation of the $LiNbO_3$ cell volume versus temperature calculated after Rietveld refinement of the neutron-diffraction patterns from the D1A neutron beamline (a); (b) shows a zoom of (a) where variation of volume of the unit cell with temperature in the range 10–110 K is displayed.

single diffraction lines of the sample, and finally, we evaluated the random effect of the line form parameters.

In Fig. 2 it is clear that the modulation in the unit-cell volume is significantly smoother than that observed in Fig. 1. This fact may be due to the larger amount of information available on D1A, since although the statistics per channel available on D1B is larger, the wider coverage in Q space of D1A compensates and permits a better determination of the cell parameters. In fact the error bars are also sensitively lower in Fig. 2 than in Fig. 1. This fact is clearly observed in Fig. 3, where we show two neutron-diffraction spectra taken from instruments D1B (a) and D1A (b). The higher amount of information available in the D1A beamline is stated by the higher number of diffraction peaks collected.

The greater amount of information collected in the diffraction patterns on D1A allowed a better evaluation of the behavior of the isotropic thermal vibrations and atomic positions of the Li, Nb, and O atoms during Rietveld treatment. Occupancy factors were fixed while isotropic vibrational factors and atomic positions were left free. Figure 4 shows the surprising and unexpected behavior observed for the Li [Fig. 4(a)] and the Nb isotropic factors [Fig. 4(b)].

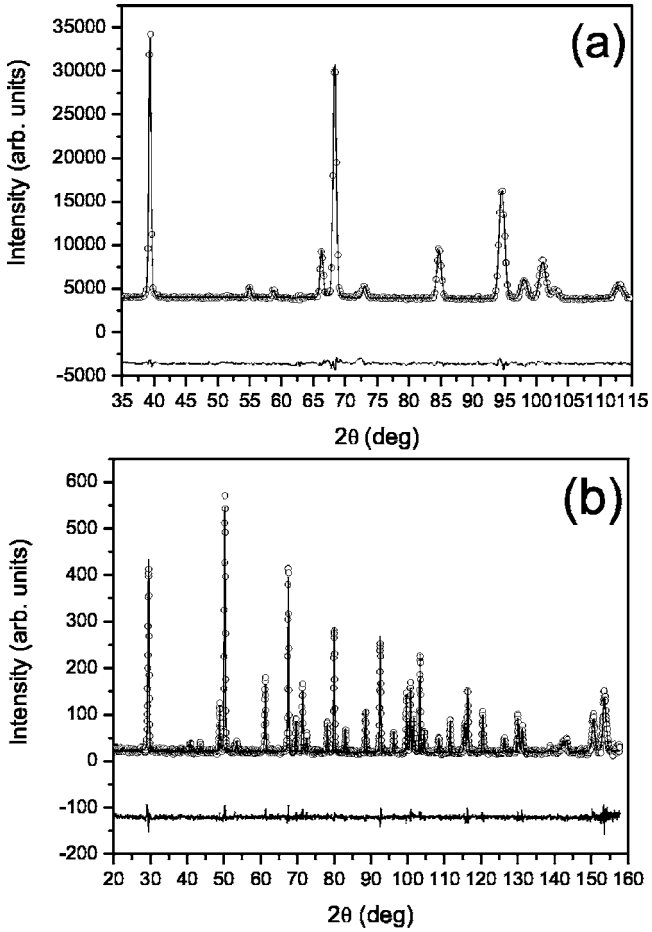

FIG. 3. (a) $LiNbO_3$ neutron-diffraction pattern obtained with the D1B beamline. (b) $LiNbO_3$ neutron-diffraction pattern obtained with the D1A beamline.

As it can be observed in Fig. 4(a), Li B_{iso} exhibits two local maximums at temperatures corresponding with the minimum in the volume of the unit cell, i.e., at 55 and 100 K. In the case of B_{iso} of Nb ions, Fig. 4(b), a local minimum at 55 K can be observed, while B_{iso} for the O atom was constant, as expected, and did not change substantially with temperature.

Following our calculations, we also evaluated the atomic positions for Li, Nb, and O atoms. Figure 5 shows the behavior observed for the Z atomic coordinates of the Li and the O atoms, corresponding to a shortening of the distance between the Li and O layers around 55 K. In contrast, X and Y atomic coordinates of O ions with temperature are constant, as expected, and do not change within error.

It is worthwhile noticing that local minima in the volume cell, as shown in Fig. 2, around 55 and 100 K, are strongly associated with the local maxima in the Li isotropic thermal factor. We expect that this fact, next to the strong reduction of the thermal vibration amplitude of the Nb atom around 55 K and the clear shortening between the Li and O layers distance in the LN cell, could be due to a LN phonon anomaly. Experiments to verify this hypothesis are in progress.

It must be emphasized that to verify the observed behavior of the lattice parameters and of the B_{iso}(Li, Nb, O) we

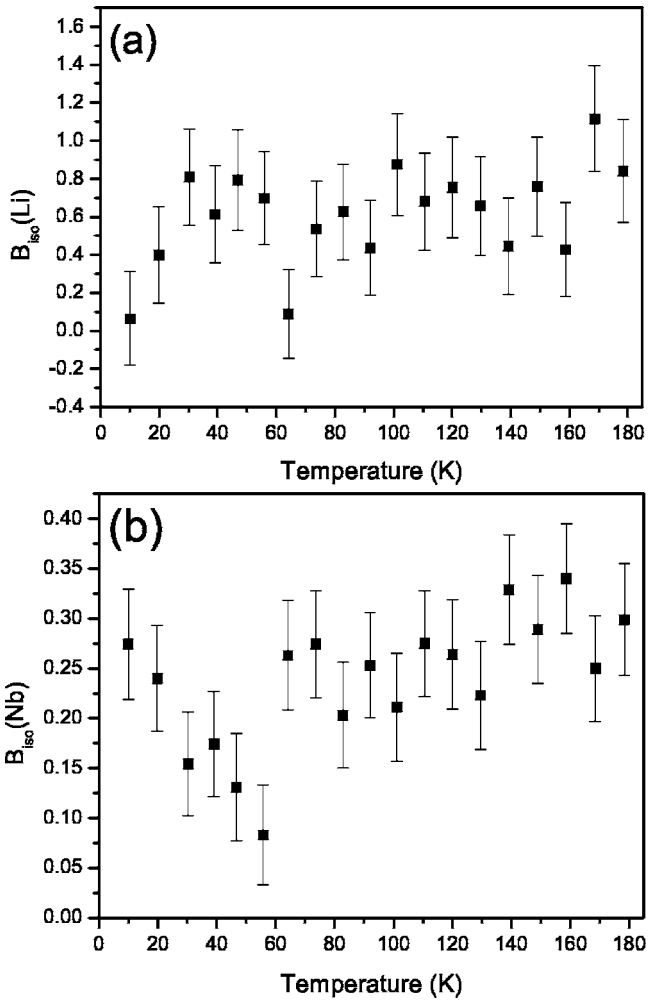

FIG. 4. Dependence of the isotropic thermal parameter for Li (a) and Nb (b) atoms with temperature (in the range 10–200 K).

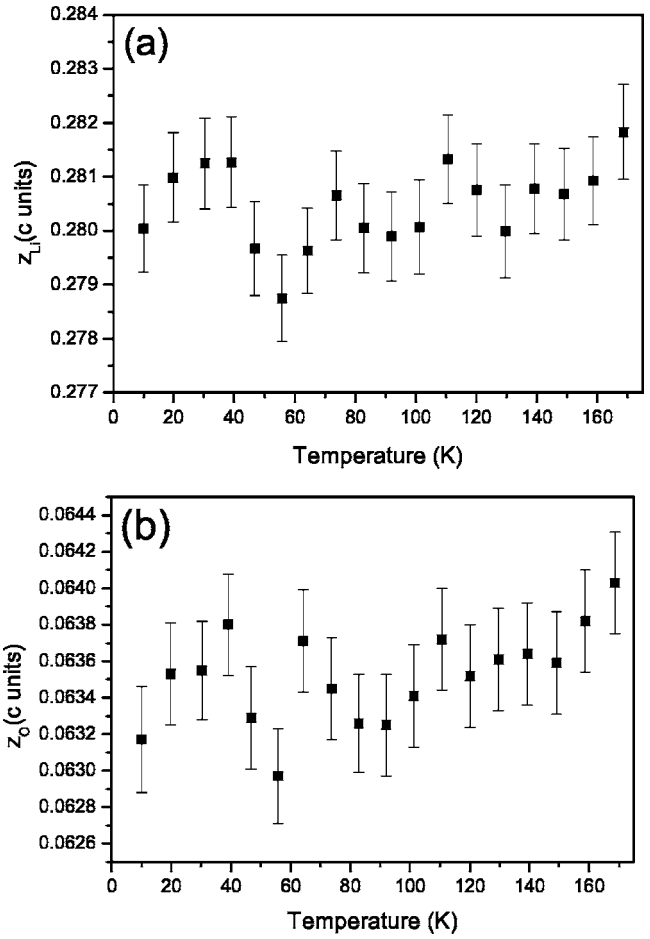

FIG. 5. Variation of the Z atomic coordinates for Li (a) and O (b) atoms with temperature in the range 10–200 K.

fixed the isothermal vibration parameters to remove the possibility of mathematical correlations during refinements. Following this procedure we could verify that there is no mathematical correlation, and the observed behavior is in fact related to the LN structure.

Observing this completely unsuspected behavior of LN structure at low temperature with a singular behavior at 55 K, and considering the shape of the volume variation with temperature, a structural anomaly is taking place around 55 K. For the moment there are no data available to exactly identify the origin (although some available measurements to identify the origin are underway). We consider that this anomaly could be characteristic of an oxygen octahedral tilt in the LN ferroelectric phase that produces a phonon anomaly, with no change in the space group, or it could be associated to a vacancy-defect ordering or moving in the LN structure. This behavior, considered as a structural anomaly, is reversible and a possible hysteresis under cycling the temperature around 55 K is being studied.

In this direction, we have estimated the spontaneous strain using the relation $s_s=2[(c-a)/(c+a)]$ (Ref. 19) versus temperature, and results are shown in Fig. 6.

As it can be observed in Fig. 6, spontaneous strain behavior presents two smooth changes in the slope of the curve. Changes in spontaneous strain are related with crystal thermal dilatation due to increasing the vibrational movement of the atoms and thus with structural changes in the crystal lattice. In our case two points are once again identified. The first one at ~55 K can be related with the shortening of the distance between the Li and O atoms, and thus with the maximum and minimum in the vibrational isotropic factor of

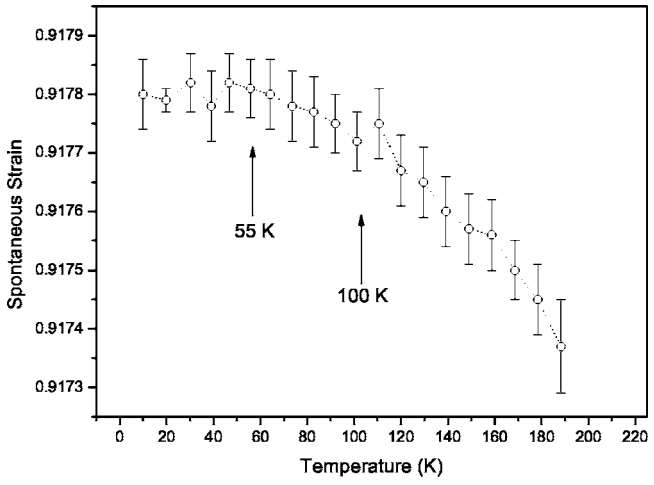

FIG. 6. Spontaneous strain versus temperature.

Li and Nb, respectively, leading to a change in the spontaneous strain. And the second one at ~100 K we think is related with changes in the thermal dilatation coefficient as it has been already explained.

Moreover, very recently Bravina *et al.*[20] have reported the existence of a singularity in the pyroelectric response of congruent LN crystals at around 60 K. They show that dielectric permittivity ε (T) dependences under cooling and subsequent heating is different at around 60 K, exhibiting a minimum in the dielectric permittivity correlated with a maximum in the amplitude of the pyroelectric response. At this temperature they also observe maxima in the pyroelectric current mode.

A careful study of Bravina's results seems to indicate that this singularity in the pyroelectric effect is strongly related with the change in the volume of the unit cell we observe. A uniform change in the crystal temperature (ΔT) produces a change in polarization given by $\Delta P_i = p_i \Delta T$, where p_i is the pyroelectric coefficient. Although it is not easy to relate a decrease in volume with the pyroelectric response, directly, when a photothermal modulation method is used (the case of Bravina *et al.*), the crystal is not clamped during measurements and then the thermal expansion is not constrained. In this case an additional effect appears, the secondary pyroelectric effect, which can be described in terms of the piezoelectric coefficient, the elastic stiffness, and the thermal-expansion coefficient.

For a constant applied electric field, $D = f_1(\varepsilon, T)$ and $\varepsilon = f_2(\sigma, T)$, which means that $dD = (\partial D/\partial \varepsilon)_T d\varepsilon + (\partial D/\partial T)_\varepsilon dT$ and $d\varepsilon = (\partial \varepsilon/\partial \sigma)_T d\sigma + (\partial \varepsilon/\partial T)_\sigma dT$. Operating and considering that the crystal is free and no stress is produced, and then $d\sigma = 0$, we obtain

$$\left(\frac{\partial D}{\partial T}\right)_\sigma = \left(\frac{\partial D}{\partial \varepsilon}\right)_T \left(\frac{\partial \varepsilon}{\partial T}\right)_\sigma + \left(\frac{\partial D}{\partial T}\right)_\varepsilon . \quad (2)$$

Equation (2) indicates that the pyroelectric effect is defined by the sum of the secondary pyroelectric effect (first term) and the first pyroelectric effect (second term). It means that when the crystal is not clamped, the additional pyroelectricity produced by the crystal deformation can be measured. In other words, when the crystal can be deformed freely, thermal expansion produces a strain, and considering the relation between ε and D, it is possible to evaluate $(\partial D/\partial \varepsilon)_T = (\partial D/\partial \sigma)_T (\partial \sigma/\partial \varepsilon)_T$, and Eq. (2) can be rewritten as

$$\left(\frac{\partial D}{\partial T}\right)_\sigma = \left(\frac{\partial D}{\partial \sigma}\right)_T \left(\frac{\partial \sigma}{\partial \varepsilon}\right)_T \left(\frac{\partial \varepsilon}{\partial T}\right)_\sigma + \left(\frac{\partial D}{\partial T}\right)_\varepsilon \quad (3)$$

and thus the secondary pyroelectric effect is described in terms of the piezoelectric coefficient, the elastic stiffness, and thermal-expansion coefficient. These terms are strongly related with changes in the spontaneous strain $s_s = KP_s^2$, where K is a constant that considers the elastics parameters.

It is important to note that our results are for a noncongruent crystal with 48.98 mol % Li while those from Bravina *et al.* are for 48.53 mol %. We have also checked what was coming out with this 48.53 mol % composition and results do not change for these two compositions (although they seem to disappear for stoichiometric compositions), but we could obtain better statistics in 48.98 mol % and so we prefer to present these data. Structural changes observed with Li content in the crystal will be published soon.

In summary, an anomalous structural modification in the LN lattice at low temperature, around 55 K, has been observed through a local change in the volume of the unit cell, a local maxima in the Li isotropic thermal factor, a local minima in the Nb isotropic thermal factor, and a shortening between the Li and O layer distance in the LN cell. This structural anomaly seems related with the thermal expansion producing a strain (which may be due to the oxygen octahedral tilting in ferroelectric phase of LN, or may be due to a vacancy-defect ordering or moving in the LN structure), which regarding the results of Bravina *et al.* seems to be able to produce an electrical displacement through ε (piezoeffect). More work is under way to exactly determine this possible explanation.

Professor J. A. Gonzalo is kindly acknowledged for useful discussions. Comunidad Autónoma de Madrid is acknowledged for partial financial support under Project No. 07N/0037/2002. Finally, D. M. M. and V. B. kindly acknowledge financial support under the Ramón y Cajal program from the Spanish Ministerio de Ciencia y Tecnología (MCyT) for the realization of this research. Part of the neutron-diffraction experiments were performed under the CRG-D1B España program of the MCyT.

*Corresponding author. Electronic address: veronica.bermudez@uam.es

[1] L. Arizmendi, Phys. Status Solidi A **201**, 253 (2004); L. Arizmendi and F. Agulló-López, Mater. Res. Bull. **XIX**, 32 (1994); J. A. Armstrong, N. Bloembergen, J. Ducuing, and P. S. Pershan, Phys. Rev. **127**, 1918 (1962); W. Sohler and F. Trager, Appl. Phys. B: Lasers Opt. **B73**, 431 (2001).

[2] S. C. Abrahams and P. Marsh, Acta Crystallogr., Sect. B: Struct. Sci. **B42**, 61 (1986); M. Veithen and Ph. Ghosez, Phys. Rev. B **65**, 214302 (2002).

[3] D. Xue and K. Kitamura, Ferroelectrics **297**, 19 (2003); Dongfeng Xue and Kenji Kitamura, J. Cryst. Growth **249**, 507 (2003).

[4] F. P. Safaryan, R. S. Feigelson, and A. M. Petrosyan, J. Appl. Phys. **85**, 12 (1999); H. Donnerberg, S. M. Tomlinson, C. R. A. Catlow, and O. F. Schirmer, Phys. Rev. B **40**, 11909 (1998).

[5] N. Zotov, H. Boysen, F. Frey, T. Metzger, and E. Born, J. Phys. Chem. Solids **55**, 145 (1994).

[6] M. R. Chowdhury, G. E. Peckman, and D. H. Saunderson, J. Phys. C **11**, 1671 (1978).

[7] A. M. Glass and M. E. Lines, Phys. Rev. B **13**, 180 (1976).

[8] S. Vieira, Phys. Rev. B **24**, 6694 (1981); Appl. Phys. Lett. **38**,

472 (1981).
[9] M. Pilar Camblor, Master's thesis, Universidad Autónoma de Madrid, Madrid, 1981.
[10] V. K. Malinovsky, A. M. Pugachev, A. P. Shebanin, and N. V. Surovtsev, Ferroelectrics **285**, 339 (2003).
[11] M. Prokhorov and Yu S. Zuz'minov, *Physics and Chemistry of Crystalline Lithium Niobate* (Adam Hilger, Bristol, 1990); A. Raüber, in *Current Topics in Material Sciences*, edited by E. Kaldis (North-Holland, Amsterdam, 1978), Vol. 1.
[12] M. D. Serrano, V. Bermúdez, L. Arizmendi, and E. Diéguez, J. Cryst. Growth **210**, 670 (2000); K. Polgar, A. Peter, L. Kovacs, G. Corradi, and Zs. Szaller, *ibid.* **177**, 211 (1997); G. I. Malovichko, V. G. Grachev, E. P. Kokanyan, O. F. Schirmer, K. Betzler, B. Gather, F. Jermann, S. Klauer, U. Schlarb, and M. Wohlecke, Appl. Phys. A: Solids Surf. **56**, 103 (1993); L. Kovacs, G. Ruschhaupt, K. Polgar, G. Corradi, and M. Wohlecke, Appl. Phys. Lett. **70**, 2801 (1997); S. Kapphan, J. Phys. Chem. Solids **52**, 797 (1991); B. C. Grabmaier, W. Wersing, and W. Koestler, J. Cryst. Growth **110**, 339 (1991).
[13] R. Fernández-Ruiz and V. Bermúdez, Chem. Mater. **16**, 3593 (2004).
[14] *The Yellow Book, Guide to Neutron Research Facilities at the ILL* (Institut Laue-Langevin, Grenoble, France, 1996), and references therein.
[15] H. M. Rietveld, Acta Crystallogr. **22**, 151 (1967).
[16] J. Rodriguez-Carvajal, *FULLPROF: A Program for Rietveld Refinement and Pattern Matching Analysis, Abstracts of the Satellite Meeting on Powder Diffraction of the XV Congress of the IUCr*, Toulouse, France, 1990, p. 127.
[17] Rietveld refinements guidelines; L. B. Mc Cusker *et al.*, J. Appl. Crystallogr. **32**, 36 (1999).
[18] G. Caglioti, A. Paoletti, and F. P. Ricci, Nucl. Instrum. **3**, 223 (1958).
[19] J. Rodríguez-Carvajal, J. L. Martínez, J. Pannetier, and R. Saez-Puche, Phys. Rev. B **38**, 7148 (1988).
[20] Svetlana L. Bravina, Anna N. Morozovska, Nicholas V. Morozovsky, and Yury A. Skryshevsky, Ferroelectrics **298**, 31 (2004).